BEHAVIOUR OF HEADED STUDS SUBJECTED TO CYCLIC SHEAR IN STEEL FRAMES WITH REINFORCED CONCRETE INFILL WALLS

L. Pallarés*[a], A. Agüero Ramon-Llin[b], J. R. Martí-Vargas[a], F. J. Pallarés[a]

[a] *Institute of Concrete Science and Technology. Universitat Politècnica de València. Camino de Vera, s/n. 46022. Valencia. Spain*

[b]*Department of Continuum Mechanics and Theory of Structures. Universitat Politècnica de València. Camino de Vera, s/n. 46022. Valencia. Spain*

Corresponding author, Associate Prof. Luis Pallarés
E-mail: lpallares@upv.es

Abstract. Headed studs are widely used to facilitate composite actions between steel and concrete structures. In steel building structures, reinforced concrete walls are commonly used to ensure composite action to stiffen steel frames as a lateral resistance system versus horizontal loads, such as earthquakes or wind. Such walls need to be anchored to the steel frame by headed studs, and these must be able to withstand shear and tension forces, as well as the interaction between these two. To design such anchors in concrete walls, it is necessary to describe experimentally their behaviour under monotonic and cyclic shear forces given that edge conditions and reinforcing details influence stud stiffness and strength.

As very few experimental studies have examined headed studs subjected to monotonic or cyclic shear with usual boundary effects in steel frames with reinforced infill walls, a new experimental test setup and test results are presented herein. Four tests on headed studs were carried out to validate the behaviour of headed studs under monotonic and cyclic shear loading, as well as to validate the new test setup.

This research shows that the behaviour of studs installed in infill walls without group effects are conservatively predicted by EC-4 and Makino's formula under monotonic shear loading. Furthermore, a reduction factor of 0.70 was found to design studs subjected to cyclic shear forces.

Keywords: Headed stud, steel frame, reinforced concrete infill wall, SRCW, stud strength, cyclic shear action, experimental behaviour.

Highlights: New test setup for headed studs installed in steel frames with reinforced concrete infill walls; four experimental test results under monotonic and cyclic shear loads are presented; experimental results are compared to provisions (EC-4, ACI318, AISC360) and authors' findings; a reduction factor is provided for cyclic shear loads versus monotonic shear loads

1. Introduction

Headed studs are widely used to facilitate composite behaviour between steel and concrete structures. Examples of composite behaviour are the reinforced concrete infill walls attached compositely (hereinafter SRCW) to steel frames around the perimeter of each wall panel (*Figure 1*) (Dall'Asta et al. [1], Morelli et al [2] and Morelli et al. [3]) or double skin composite shear walls (Zhang et al. [4] and Yan et al. [5]). Currently, concrete walls are designed to stiffen steel frames subjected to horizontal loads, such as earthquakes or wind, as a primary lateral resistance system for building structures (Peng and Gu [6], Naseri and Behfarnia [7]). Such walls will be anchored to a steel frame with headed studs that must withstand shear and tension forces (AISC360 [8] and Yan et al. [9]).

During an earthquake, headed studs in SRCW must withstand alternate shear forces, and many variables, such as cracks or free edges in concrete located in the vicinity of the headed stud (*Figure 2*), may influence their behaviour.

Firstly, from the point of view of the Serviceability Limit State, SRCW are deformed (*Figure 2*) under a horizontal load and the concrete wall compositely acts with the steel frame through the headed studs subjected to shear and tension stresses. In this situation, the shear stiffness of the headed studs performs a vital role to achieve the stiffening effect of the wall. Longitudinal cracks due to splitting may appear and affect the stiffness of the headed studs.

Furthermore, from the point of view of the Ultimate Limit State, the possible modes of failure with the edge conditions of the SRCW may occur in the steel or in the concrete located in the vicinity of the studs (pryout failure following the terminology of ACI318 [10] or CEB [11]). The detachment of the concrete wedge (breakout failure in ACI318 [10] and CEB [11]) is prevented thanks to the presence of the stirrups.

Thus, to design headed studs installed in SRCW, it is necessary to know their behaviour under monotonic and cyclic shear loading with the proper boundary conditions of SRCW.

Pallarés and Hajjar [12] conducted an in-depth literature review on 391 tests with headed studs subjected to monotonic and cyclic shear and analysed modes of failures, and assessed different formulae to design anchors, to later propose design formulae. Many studies have been conducted on headed studs subjected to monotonic forces, as stated by Pallarés and Hajjar [12], but research on headed studs with particular boundary conditions of SRCW and cyclic loading, is lacking in the literature.

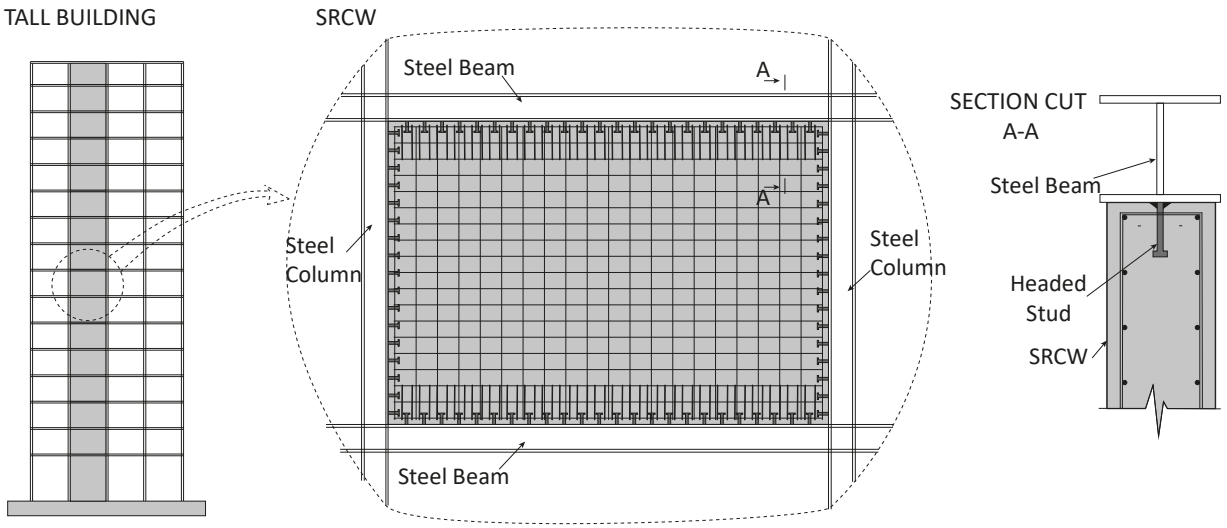

Figure 1. SRCW and details of headed studs and reinforcement.

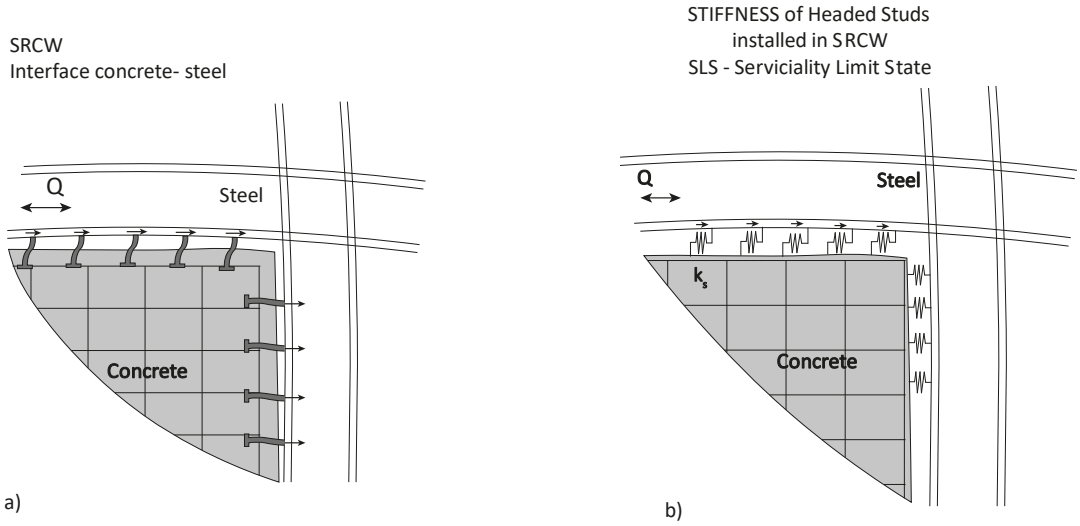

Figure 2. a) Detail of deformed shape of SRCW, b) Spring which models the interaction between concrete and steel in SRCW.

A new test setup that allows for replication of particular conditions in SRCW is proposed. The new test setup presented in this work is used to describe the behaviour of headed studs under cyclic and monotonic shear loading, edge conditions of infill walls and, optionally, it considers the group effects of headed studs (Spremic et al., [25]), by eliminating the disadvantages of push-out tests. The results from four tests are reported to validate the testing procedure and to be compared with the provisions (EC-4 [26], ACI318 [10], AISC360 [8]) and other authors' findings.

2. Material and methods

Headed studs are steel anchors that fulfil the requirements established in AISC360 [8], and these are anchored to a steel plate before pouring concrete. The geometric dimensions of headed studs are described in *Figure 3*. These studs are identified by the main dimensions, namely, shank diameter (d) and height (h). Another relevant length is h_{ef}, or effective height, which is the embedded length from underneath the head to the concrete surface.

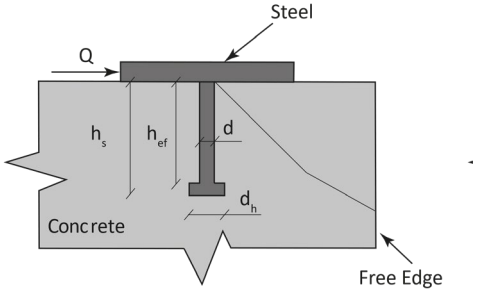

Figure 3. Geometric dimensions of a headed stud.

The steel frame machine and test setup, including the variables considered for the four specific specimens, are described below.

2.1 Test setup

In relation to the existing test setups on headed studs subjected to cyclic shear loads, Hawkins and Mitchell [13], Gattesco and Giuriani [14], Bursi and Ballerini [15], Zandonini and Bursi [16], Civjan and Singh [17] and Fa-xing et al. [18] performed different types of push-pull tests on shear connectors under high amplitude cyclic (seismic) shear loading for slabs in composite beams with no edge conditions. By contrast, the push-out test (from Viest [19] up to Jianin et al. [20] or Yu-Liang et al. [21]) or "in the field" (*Figure 4*) are the most common test configurations

used for headed studs or shear connectors, in general (Shariati et al. [22], Shariati et al. [23] and Bezerra et al. [24]). Nevertheless, the push-out test might not represent pure shear tests in headed studs due to the eccentricity of the load (Civjan and Singh, 2003 [17]) introduced during the test as seen in *Figure 4*. Zhuang and Liu [4] fixed this issue with a test setup that minimized the load eccentricity during the test procedure. In spite of this new test setup, the push-out test configuration does not allow for edge conditions, reinforcing detailing or the interaction loads of shear and tension of SRCW to be tested.

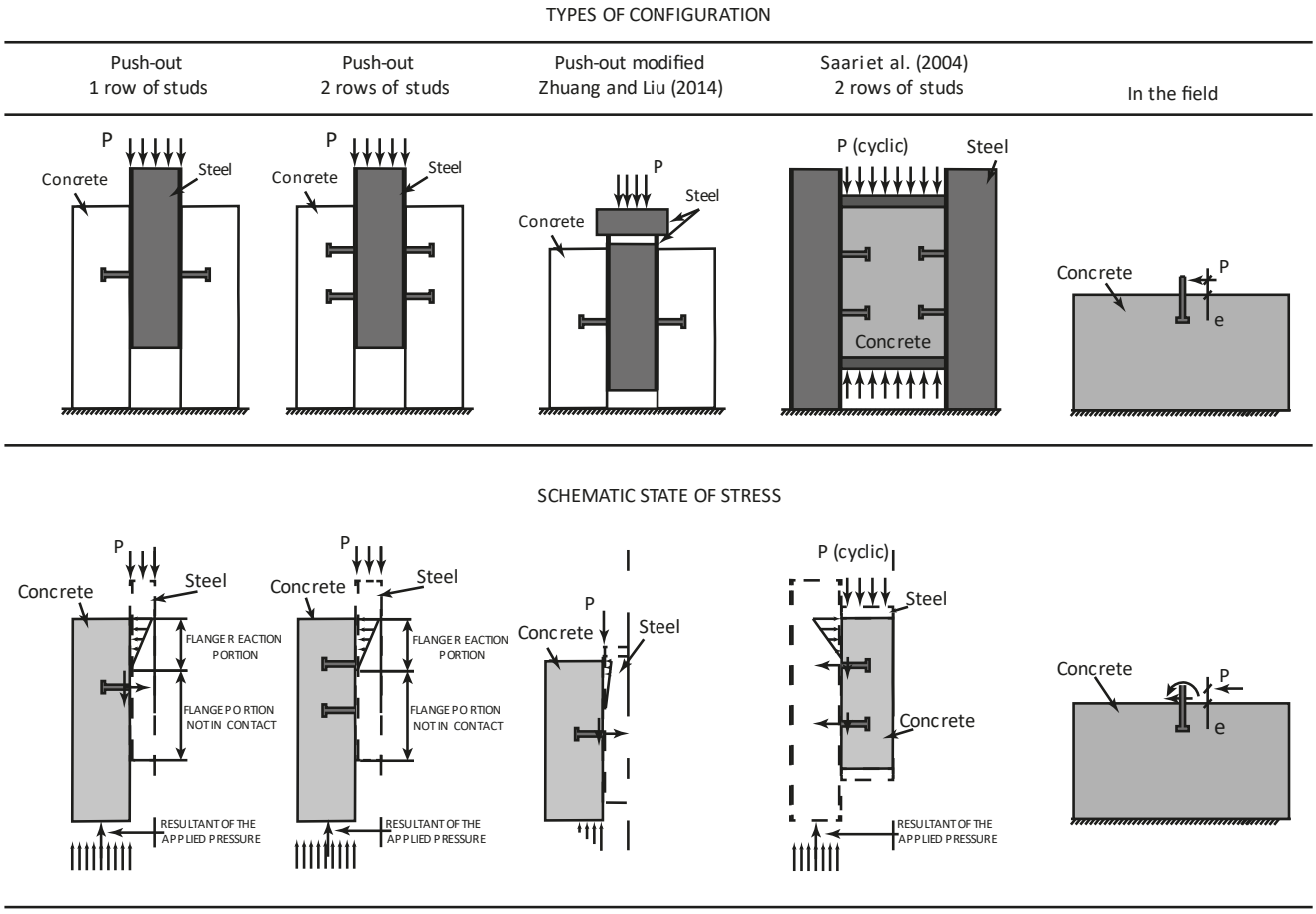

Figure 4. Test configurations for the shear loading of headed studs.

A new reaction steel self-supporting frame was designed to test a headed stud welded to a piece of steel beam (IPE 200 in *Figure 5*) and embedded in a parallel-piped reinforced concrete (RC) specimen. This specimen was intended to represent local behaviour on a full scale of the shear stud connection in SRCW. A hydraulic actuator (1000kN capacity) was horizontally located on the steel frame and equipped with a HBM U10 tension-compression load cell within the 500kN range. Next to the load cell was a pin connection that was free to rotate on the plane of specimen and was bolted to the testing machine. The pin was connected to a collar that wrapped the steel beam at both ends. A threaded rod system was used to fully accommodate reversed shear loading. Two steel blocks (*Figure 5*) were located between the steel beam and the collar. As the load action line of the actuator was 1 mm above the steel and concrete interface (*Figure 5*), shear force prevailed over both flexure and tension in the headed studs. This configuration also allowed the anchors to be tested under tension and shear forces by hanging an actuator over the upper beam of the reaction steel frame. The reaction steel frame is shown in *Figure 6*.

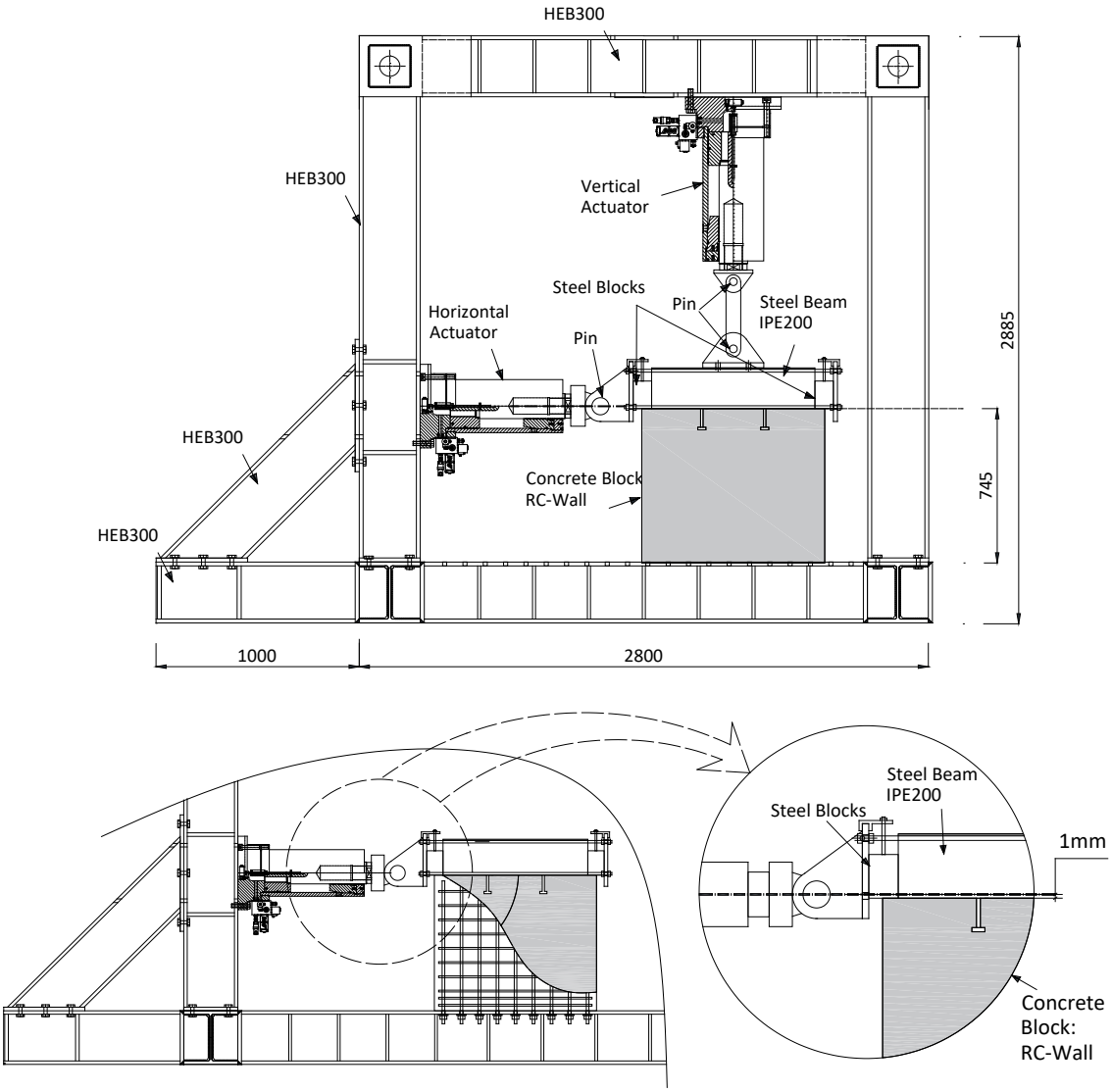

Figure 5. Test layout for SRCW.

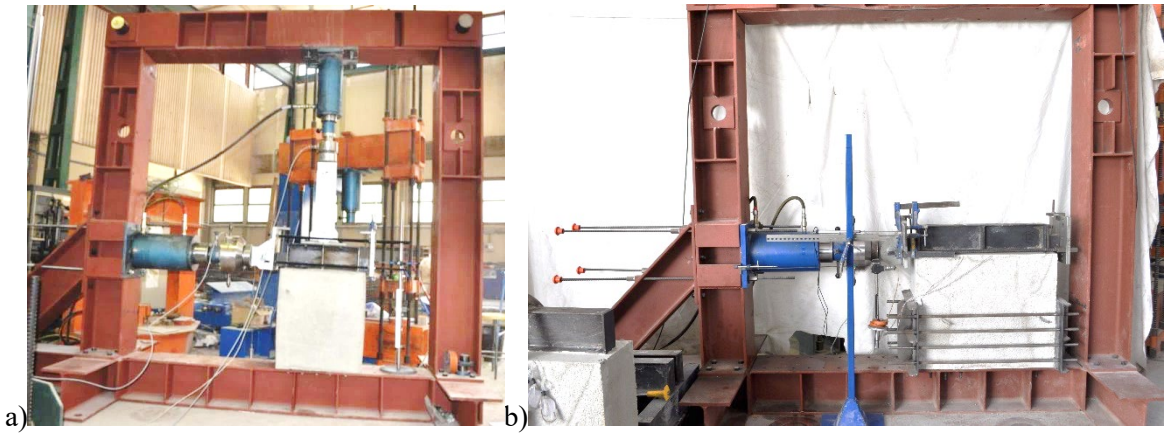

Figure 6. a) Test setup for the headed studs in the reinforced concrete panels subjected to a) shear and tension forces, b) subjected to shear forces.

2.2 Specimens and variables

The specimen was created with a piece of IPE200 steel beam (820 mm long), where headed studs were welded according to the test configuration proposed for each specimen (*Figure 7.a*). Once studs were welded, they were encased in the specimen steel reinforcement and placed in moulds (*Figure 7.b*) to pour concrete (*Figure 7.c*).

Figure 7. Specimen production. a) steel beam with welded headed stud anchors, b) reinforcement of the specimens and steel form, c) specimen after the concrete was poured.

The concrete block of the specimen was 745 mm high with dimensions 300x900mm from the top view (*Figure 8*). All the headed stud anchors tested herein had enough development length (h_{ef}/d=4.74) under shear force to achieve ductile failure (h_{ef}/d=> 4.5) in steel by avoiding brittle failures in concrete, such as pryout failure, as defined in ACI318 [10] and CEB [11]. A shank diameter of 19mm was selected for specimens. Reinforced detailing was provided in the concrete block to prevent concrete breakout failures according to ACI318 [10], similar to reinforcing in SRCW.

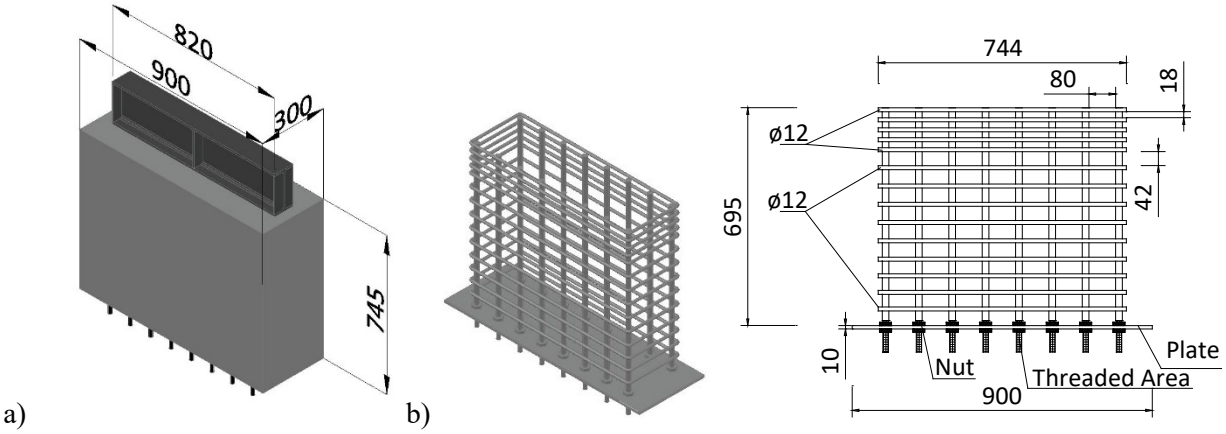

Figure 8. a) Dimensions of specimens, b) steel cage (in mm).

This concrete block was able to simulate a stretch of a concrete wall with embedded steel anchors and a high density of stirrups on the upper side to control breakout failure. The number of arranged stirrups was such that their mechanical capacity exceeded the shear strength of the headed studs.

The specimens were monotonically and cyclic shear loaded, and the following variables were considered:

- The diameter (d) and height (h_{ef}) of the headed studs, being 19mm the shank diameter and 90mm the effective height, which gave a ratio of effective height to diameter (h_{ef}/d), equal to 4.74.

- Depending on the number of studs and distances between them, the following layouts were proposed:

  a. *Single Stud (SS)*. A single stud was located in the centre of the steel beam (*Figure 9.a*).

b. *Single row of studs without group effects* (SRS). In order to avoid group effects related to pryout failure in accordance with ACI318 [10] and CEB [11], a separation of at least $3 \cdot h_{ef}$ between studs was selected for each specimen. A distance of 300mm between studs in the load direction was configured to reach no group effects.

Table 1 lists the nomenclature, the number of studs, the stud layout on the steel beam for each specimen and the type of load.

Table 1. Nomenclature and properties of the specimens.

Specimen	Number of headed studs	Stud Layout	Monotonic/ Cyclic
1sM	1	SS	M
2sM	2	SRS	M
1sC	1	SS	C
2sC	2	SRS	C

The amount of materials used to prepare each specimen is specified in *Table 2*.

Table 2. Material needed to manufacture a specimen.

Concrete	0.201m^3
Steel cage	12 bars of ϕ16mm, 735 mm long 14 stirrups of ϕ12mm and 744x240 mm 24 nuts
Steel Beam	IPE 200 m, 820 mm long
Studs	Number of studs according to the test

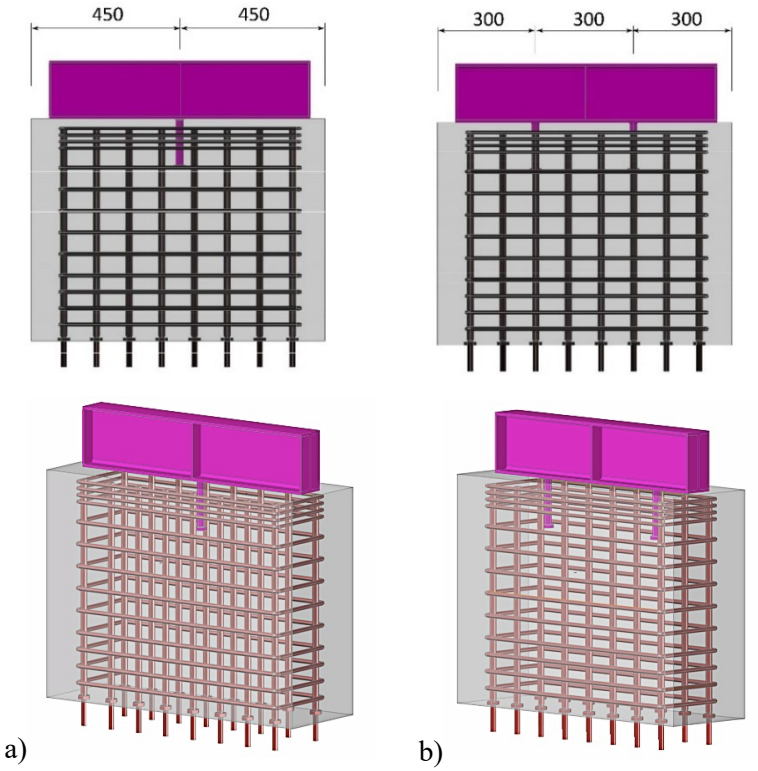

Figure 9. a) SS layout, b) SRS layout (in mm).

2.3 Materials

a. ***Concrete:*** Two concrete cylinder specimens (150mm in diameter and 300mm high) were cast to determine concrete strength for each batch. Specimens 1sM, 1sC and 2sC were cast in the first batch, and 2sM was cast in the second batch. Concrete strength varied from 24.5 (first batch) to 41.4MPa (second batch).

b. ***Steel of headed studs:*** the properties of the steel provided by the manufacturer are shown in *Table 3*: type of steel, ultimate stress of steel (f_u), yield stress of steel (f_y), composition and resistance features.

Two tension tests were carried out on 19-mm diameter studs welded to a metal profile (*Figure 10.a*). Each stud was instrumented with two strain gauges. An ultimate stress of 537.1MPa (152.3kN) and 534.3MPa (151.5kN) was attained for each stud. The strain at peak load reached $20 \cdot 10^3$ με approximately in both tests. Besides, a change occurred in the slope on the curve for a load of 130kN which indicated the yield limit stress, that had an equivalent stress value of 458MPa (*Figure 10.b*) for a strain of $2.29 \cdot 10^3$ με.

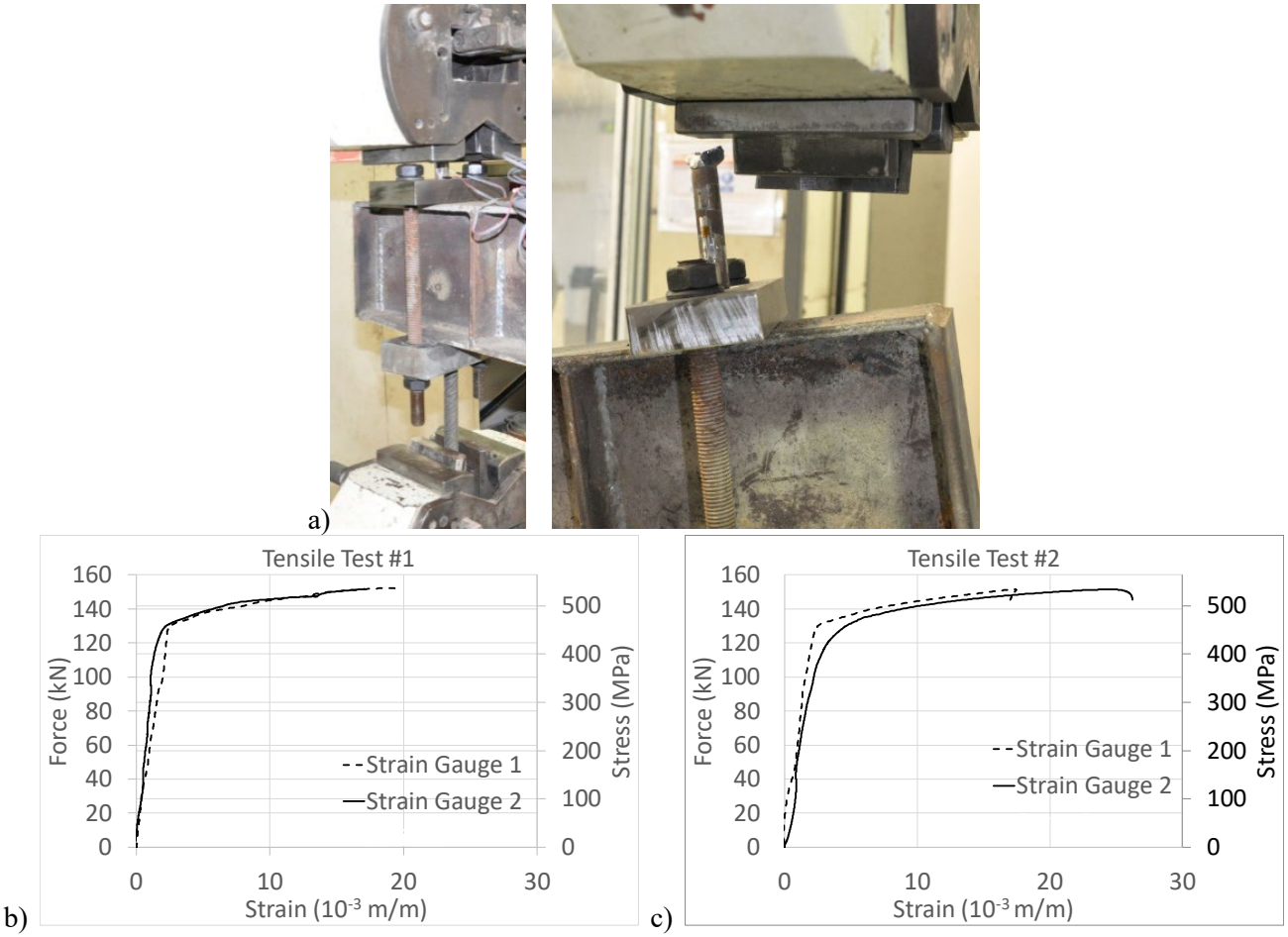

Figure 10.a) Tensile test of stud, b) tensile test #1. Peak load: 152.29kN (537.1MPa), c) tensile test #2. Peak load: 151.50kN (534.3MPa).

Besides tension strength, one shear test of a stud was carried out with a double shear plane (*Figure 11.a*) and the ultimate load attained was 221.5kN (*Figure 11.b*). Then, each cross section carried 110.75kN, which represented approximately 72% of the tensile strength.

a) 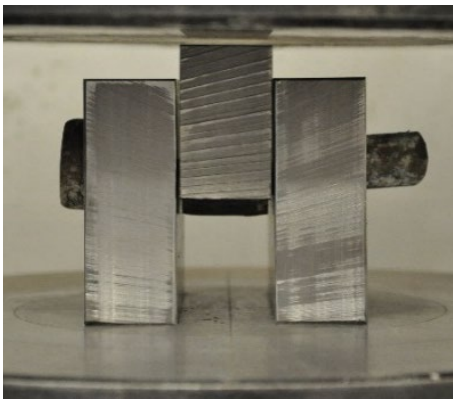 b) 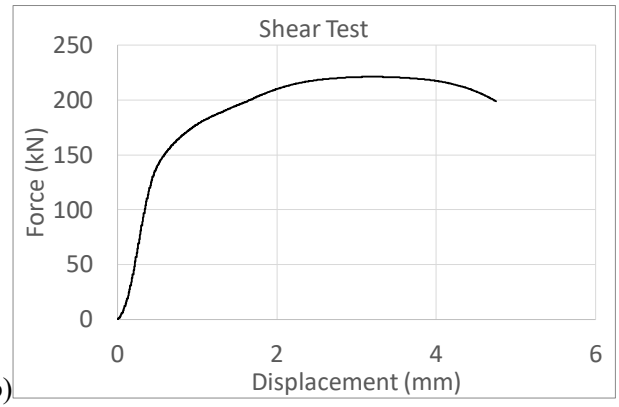

Figure 11. Shear test results. (ϕ=19mm). a) Test Setup. b) Results with peak load at 221.25kN.

Table 3. Steel properties of headed studs.

Steel	f_u (MPa)	f_y (MPa)	Composition	Strength Characteristics
S35J2G3	450	450	ETA-03/0039	EN 10025:2005

2.4 Test Procedure and Instrumentation

After the specimen was anchored to the reaction steel frame, a PC was programmed to run the test under displacement control. Two test procedure types were run: i) monotonic tests with a constant velocity of 0.1 mm/s, imposed up to failure; ii) a cyclic test according to the procedure based on (Krawinkler et al., [27]) and FEMA-461 [28]).

The cyclic shear load application was performed under displacement control, and slip targets were used from the time the test started. Each displacement step presented three substeps, where the magnitude of displacement (a_i) and velocity remained constant (*Figure 12*). Equations (1) and (2) governed the test procedure:

$$a_{i+1} = 1 + a_i \quad where\ a_1 = 1\ mm \tag{1}$$

$$T_{i+1} = 40 + T_i \quad where\ \ T_1 = 40\ s \tag{2}$$

An HBM U10M of the 500kN tension-compression range cell-load was located between the actuator and the specimen. An LVDT was located on the opposite side of the actuator to measure the slip between the steel beam and the concrete block.

When instrumentation ended, strain gauges were placed at the mid-height of the stud to measure the strains along the studs (*Figure 13*). HBM-type LY41 strain gauges (3 mm grid length and 120 ohms electrical resistance) were glued onto the studs. Strain gauges measured strains in the axis direction. To this end, the level of anchor of stud and the mode of failure could be determined from the strains.

Figure 12. Test procedure under displacement control.

Figure 13. Strain gauge at the mid-height of studs.

3. Results and Discussion

3.1 Modes of failure.

Modes of failure that can occur in studs installed in SRCWs may happen in concrete, steel, or mixed in concrete and steel. Concrete failure can occur in two ways: i) by breakout, that consist of a development of a breakout prism due to a free edge (*Figure 14.a*); ii) by pryout that consist of failure of concrete in the vicinity of the headed stud (*Figure 14.b*). Concrete breakout failure may be restrained with appropriate anchor reinforcement like the one located in the specimen.

The failure in the steel (*Figure 14.c*) can be detected by visual inspection observing a shear rupture in the section of steel or through the strain measurement of gauges glued to the shank of the stud. If the strain recorded by the strain gage exceeds the value of the yield strain ($>2.29 \cdot 10^3 \mu\varepsilon$) with no degradation observed in the concrete, the stud is considered to have failed in the steel.

Finally, if the strain in the steel reaches its plateau in the load-strain curve and a significant degradation of the concrete is observed, a mixed failure is considered.

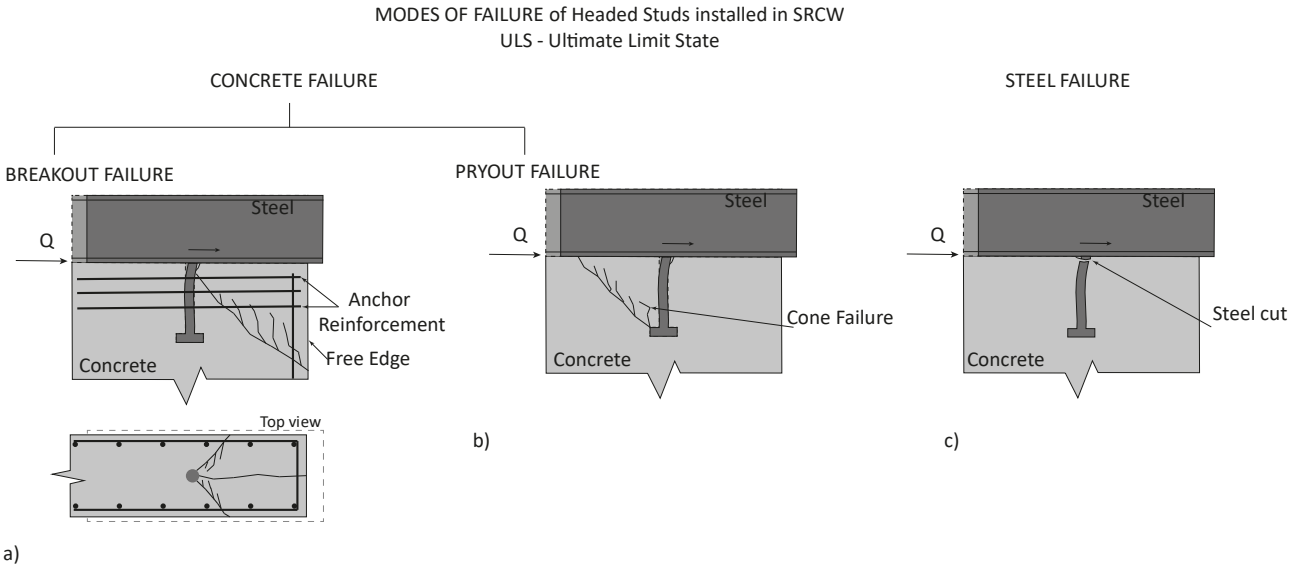

Figure 14) Modes of failure in studs installed in in SRCW. a) Breakout. b) Pryout. c) Steel.

Based on the pictures in *Figure 15*, specimen 1sM (*Figure 15.a*) had a mixed failure of steel and concrete. The stud bent and presented large strains in the shank without rupture of the section and exhibited remarkable degradation in the concrete. At the joint section between the anchor and the steel beam, the stud was subjected to tension and shear since the concrete in its vicinity had cracked.

Figure 15. Specimens at peak load: a) specimen 1sM; b) specimen 2sM; c) specimen 1sC; d) specimen 2sC.

The same failure type occurred in specimen 2sM (*Figure 15.b*), in which a sudden drop occurred after the peak because both concrete and one of the steel studs failed. In this test, failure was caused by the brittle failure of the

concrete located in the vicinity of one of the studs. This was because, despite arranging the studs at a distance greater than $3h_{ef}$, loads were concentrated in the vicinity of the concrete of one of the studs and this causes a failure due to concrete cracking, as seen in the existing cracks (*Figure 15.b*) that reached the lateral edges of the wall. This crack type also appeared in the test carried out with the two studs subjected to cyclic stresses 2sC (in both load directions). Thus, a clear group effect appears and tends to cause failures by breakout, which can be restricted by the reinforcing stirrups arranged at the top.

In the cyclic tests, the specimen 1sC, with one stud, showed clear failure by the shear in steel. In the specimen with two studs (2sC), longitudinal cracks appeared in the concrete; these reached the lateral edges of the wall, although failure also occurred in the steel of the studs. Thus, a failure mode in steel was clearly observed in both cyclic tests. This was due to the successive cycles that generated steel degradation in concentric circles of the steel section: these circles reduced the strength capacity of steel as well as caused the final failure of the stud.

No test showed failure by breakout or side blowout, which confirmed that the reinforcing details in the form of stirrups were effective to avoid these failure types. Tests were run with two headed studs separated from one another by a distance greater than $3h_{ef}$, and the peak experimental loads were twice the configuration with one stud only, which indicates that there were no group effects.

3.2 Load-slip curves

The load-slip curve was idealized by a curve (*Figure 16*), on which the key parameters for its definition were established from the experimental curve. The key parameters used to evaluate the performance of the monotonic and cyclic specimens were two, following Wang et al. [29]: peak strength (Q_n) and ductility index (μ). Shear stud ductility can be calculated as Equation 3:

$$\mu = \Delta_u/\Delta_y \tag{3}$$

where Δ_y and Δ_u are defined as the slips at which stud strength increases or reduces to 95% of the stud's peak strength, respectively (Burnet and Oehlers [30]). *Figure 16* represents the values of Δ_u in the case of a ductile failure ($\Delta_{u,d}$) and in the case of a brittle failure ($\Delta_{u,b}$) from which it can be deduced that the index ductility is higher in the case of ductile failures than in the case of brittle failures.

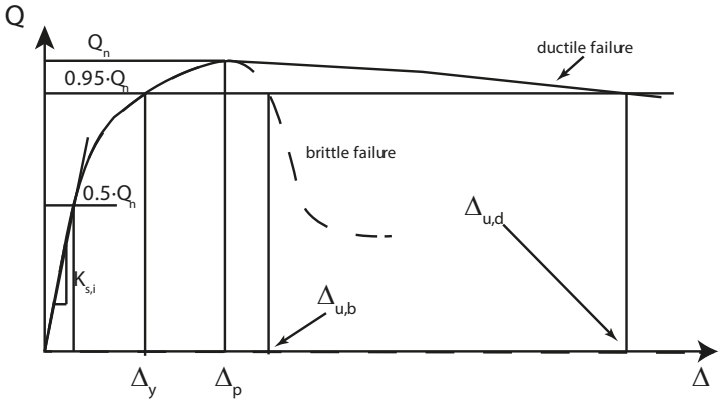

Figure 16. Idealized load-slip curve of brittle and ductile failure under monotonic shear loading.

Tables 4 and *5* summarize the experimental results of the monotonic and cyclic specimens.

Table 4. Experimental Results in the Monotonic Tests.

	Q_{test} (kN)	Δ_p (mm)	Δ_y (mm)	Δ_u (mm)	μ	Type of failure
1sM	97.71	11.23	7.35	13.52	1.84	Mixed
2sM	196.07	7.36	6.72	7.53	1.12	Mixed

The results of the cyclic tests were computed with the cyclic backbone curves in both loading directions.

Table 5. Experimental Results in the Cyclic Tests.

Positive Cyclic Loading						
	Q_{test} (kN)	Δ_p (mm)	Δ_y (mm)	Δ_u (mm)	μ	Failure type
1sC	65.96	5.87	4.31	6.31	1.46	S
2sC	140.3	9.01	7.75	9.61	1.23	Mixed
Negative Cyclic Loading						
	Q_{test} (kN)	Δ_p (mm)	Δ_y (mm)	Δ_u (mm)	μ	Failure type
1sC	67.3	5.86	3.86	6.42	1.66	S
2sC	130.6	8.95	7.09	9.61	1.35	Mixed

The experimental curves for the performed monotonic and cyclic tests are given in *Figure 17*.

The 1sM test (*Figure 17.a*) showed a typical load-slip curve of the tests with ductile steel failure. It had a high ductility index (μ=1.84) compared to the index (μ=1.12) of the load-slip curve of the two headed studs. In 2sM test, despite the separation was greater than that prescribed by ACI318 [10] and CEB [11] to avoid group effects, ductility was less compared to single stud layout given the edge effects that appear in the concrete block.

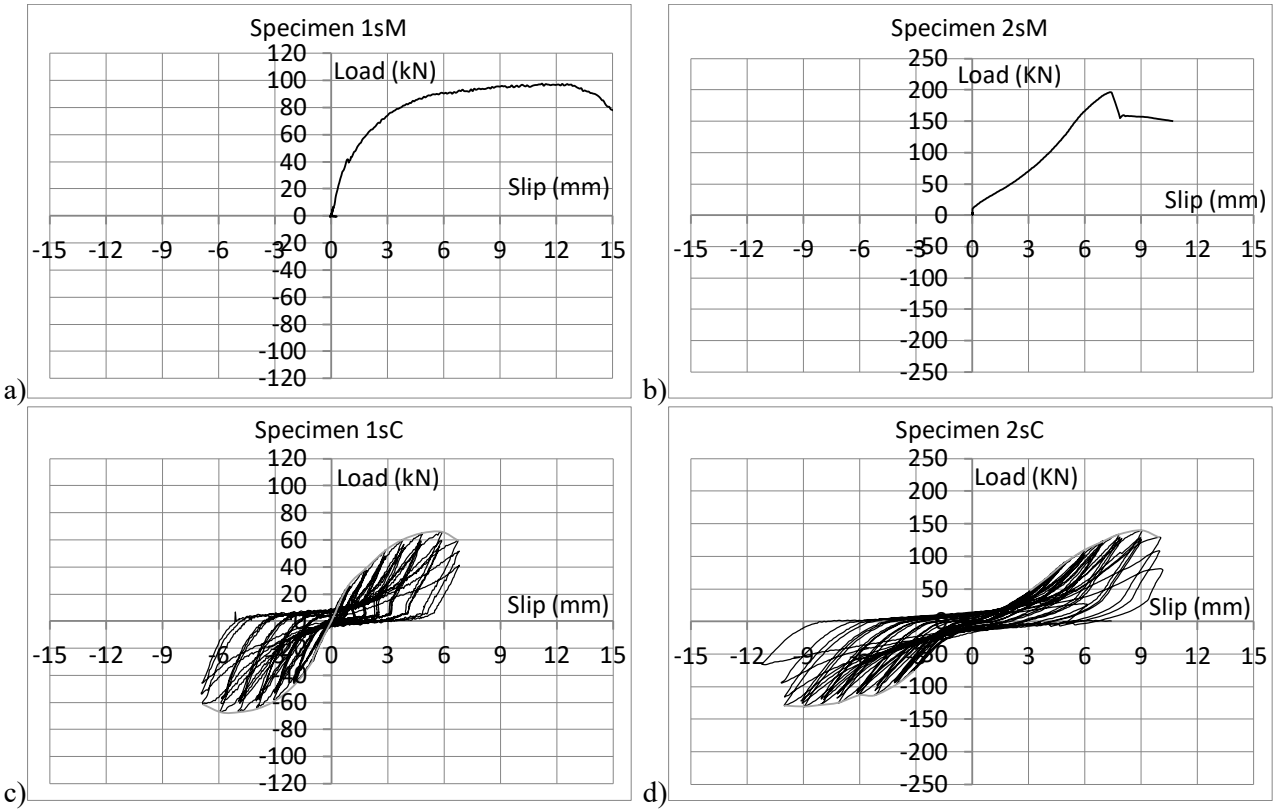

Figure 17. Load slip curves for: a) specimen 1sM; b) specimen 2sM; c) specimen 1sC; d) specimen 2sC.

In the monotonic tests, there were fewer displacements for the maximum load in the arrangement with two studs (2sM) than in that with one stud (1sM) because the maximum load was determined by the failure of the concrete in

the former and by steel in the latter. By contrast, the cyclic tests involved greater displacement for the maximum load specimen with two studs (2sC) as they required a more marked concrete degradation to achieve a higher ultimate load.

3.2 Load-strain curves

In regard to the measures with strain gauges, the strains in the monotonic tests reached the yield point (*Figures 18.a* and *18.b*). The stud was bent until the surrounding concrete pulled up (*Figure 15*) and the yield point was reached. In specimen 2sM, cast with a concrete strength of 41.4MPa, the concrete sufficiently anchored one of the headed studs and reached a strain of $1.95 \cdot 10^3$ με in the shank at the peak load of 196.07kN. At this load level, sudden concrete failure occurred in the vicinity of the headed stud, and a sharp drop appeared on the load-displacement curve. Specimen 1sM, with lower concrete strength (24.5MPa), showed progressive failure, as indicated by the soft slope of the load-deformation curve after the peak (*Figure 17.a*).

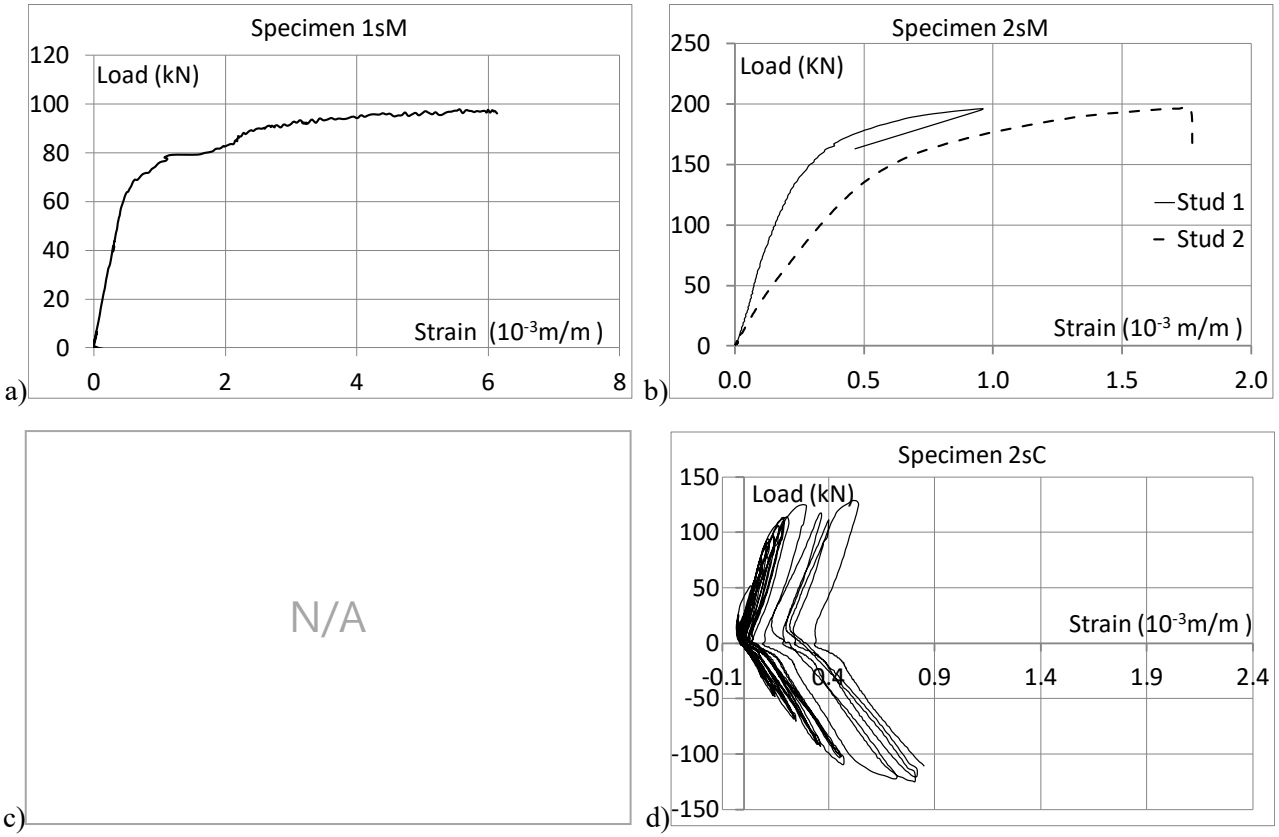

Figure 18. Load versus strains in headed studs of specimens: a)1sM; b)2sM; c)1sC and d)2sC.

The strains recorded in the strain gauges during the cyclic tests were erratic in specimen 1sC due to problems on the contact surface of the gauges, and a maximum strain of $0.8 \cdot 10^3$ με in the headed stud was recorded (no figure is included). This specimen did not have any crack type in the concrete as the stud was perfectly anchored to the shear load and its tension strains were irrelevant. In specimen 2sC, one of the studs showed strains below $1 \cdot 10^3$ με, while the other headed studs displayed larger strains (*Figure 18.d*), which demonstrates plastic deformation due to tension and the lack of anchorage to the shear load. The concrete in the vicinity (*Figure 15.d*) showed some degradation and longitudinal cracks opened, which allowed the stud to enter in tension (*Figure 18.b*). Therefore, the two studs located in a row in a SRCW were subject to group effects, even when separated by more than $3h_{ef}$.

3.3 Stiffness

Oehlers and Coughlan [31] conducted a statistical analysis of load-slip curves with 116 push-out tests in which concrete slabs did not fail prematurely. These authors recommended the equations shown in *Table 6* to estimate stiffness and suggested estimating the mean initial tangent stiffness, K_s, as the stiffness at $0.5 \cdot Q_n$ (*Figure 16*).

Table 6. Proposals of stud stiffness.

Stiffness	Oehlers and Coughlan [31]	Ollgaard et al. [32]	Ann and Cerdewall [33]	Buttry [36]
K_s	$\frac{Q_n}{d(0.16 - 0.0017 f_c)}$	$Q_n(1 - e^{-18\Delta})^{2/5}$	$Q_n \frac{2.24 \cdot (\Delta - 0.058)}{1 + 1.98 \cdot (\Delta - 0.058)}$	$Q_n \frac{80 \cdot \Delta}{1 + 80 \cdot \Delta}$

In the approaches of Ollgaard et al. [32] as well as Ann and Cederwall [33], load-slip curves are described by the functions given in *Table 6*, which presents an ascending branch, even after shear strength is reached.

More recently, Xue et al. [34] and Wang et al. [35] proposed formulae to predict shear load-slip curves based on new push-out tests where, once again, the ductile behaviour of studs was ensured. As indicated by Classen and Hegger [37], these approaches are suitable only to describe the ductile behaviour of shear studs, with no descending shear-slip branch. None of these models allowed for stud deformation capacity to be determined and none were able to predict the pryout or breakout failure restrained by stirrups that may occur in SRCW.

For cyclic loading shear, Buttry [36] (*Table 6*) proposed an empirical formula to predict the load-slip relation under the reloading condition in push-out tests. Oehlers and Coughlan [31] tested eight push specimens under cyclic loadings and found that load-slip paths varied from the static case because of permanent concrete deformation.

In the specimens with only one stud, the monotonic test (1sM) presented an initial stiffness of 38.5kN/mm (*Table 7*), which was 51% higher than the cyclic test (1sC) (25.5kN/mm is the average stiffness of both positive and negative curves) if the backbone curve was used for testing.

In the specimens with two studs, and despite avoiding the group effects by separating studs by more than $3h_{ef}$ (in accordance with ACI318 [10]), it was evident that concrete cracking caused by edge conditions of SRCW influenced the deformational behaviour of the studs. Tests 2sM and 2sC resulted in less stiffness (24.2kN/mm and 20.6kN/mm,) than that obtained in the tests with one stud (38.5kN/mm and 25.5kN/mm). The load to move two studs caused splitting cracks in the concrete that were restricted by the stirrups located on the upper head (*Figure 15*) and, the sum of the stiffness of studs caused the concrete to crack, which also resulted in loss of stiffness in relation to the single stud tests.

Table 7. Stiffness of specimens (K_s in kN/mm).

	Experimental Test	Oehlers and Coughlan [31]	Ollgaard et al.[32]	Ann and Cerdewall [33]	Buttry [36]
1sM	38.5	32.1	77.5	61.8	76.8
2sM	24.2	64.5	48.4	48.6	48.2
1sC*	23.5/27.4 Avg. 25.5	22.2**	47.9**	39.5**	47.5
2sC*	17.0/24.2 Avg. 20.6	46.2**	48.4**	46.5**	48.2

* Applied to positive/negative.
** Estimates for the monotonic load test.

In general, the stiffness reported by Ollgaard et al. [32], Oehlers and Coughlan [31] and Ann and Cederwall [33] duplicated the stiffness values experimentally obtained in the test proposed under the SRCW edge conditions. Classen and Hegger [37] stated that generally all models neglected major influences and considered too few

parameters. These models are based on push-out tests in which only shank failure (in slender studs) or pryout failure (in stocky studs) is possible. The proposed test setup in the present study properly captured the load-slip curve of studs when the breakout failure restrained by hairpins, steel failure or pryout failure occurred as in SRCW. Therefore, a model with a post-peak descending branch as a multilinear approach of the shear-slip curve, similar to Classen and Hegger [37] or Wang et al. [35], was necessary to fully describe the behaviour of the studs installed in SRCW.

Since only four tests have been carried out to date, it is not possible to provide an expression for these structural elements, but they do halve the values obtained with current expressions.

In the cyclic tests, the expression of Buttry [36] duplicated the stiffness of the embedded studs in SRCW. This is because his proposal was based on push-out tests that did not include the edge conditions of these structural components.

3.4 Strength Provisions

ACI318 [10] and CEB [11] included a set of equations for the strength of anchors. Provisions are complex, and only concrete pryout failure (Q_{cp}), as a local failure in the vicinity of the anchor due to shear loading and steel failure, is considered herein for members with composite action. ACI318 [10] and CEB [11] included several other failure modes, such as breakout or side blowout, but they are irrelevant here because reinforcement (hairpins and stirrups) is detailed in the test to preclude such failure modes. Then, the pryout prediction by ACI318 [10] and CEB [11] is:

$$Q_{cp} = k_{cp} \cdot N_{cb} \tag{4}$$

where:

$k_{cp} = 2$ if $h_{ef} \geq 2.5$ in

$N_{cb} = \frac{A_{nc}}{A_{nco}} \cdot \Psi_{ec,N} \cdot \Psi_{ed,N} \cdot \Psi_{c,N} \cdot \Psi_{cp,N} \cdot N_b$ is the concrete breakout strength for a group of anchors;

$\Psi_{ec,N}$ is the modification factor for the anchor groups loaded eccentrically in tension. In this case, they are loaded centrically, so this factor is 1.

$\Psi_{ed,N} = 0.7 + 0.3 \cdot \frac{C_{a,min}}{1.5 * h_{ef}} \leq 1$ is the modification factor for edge effects and $c_{a,min}$ is the minimum edge distance.

$\Psi_{c,N} = 1.25$, for cast-in anchors, is the factor used to consider cracking.

$\Psi_{cp,N} = 1$ for cast-in anchors where supplementary reinforcement is provided to control splitting or in the areas with present concrete cracking.

$N_b = k_c * \lambda * \sqrt{f_c'} * {h_{ef}}^{1.5}$ where $k_c = 24$ for casting in place anchors.

λ is the modification factor for lightweight concrete. It equals 1 in normal concrete.

$A_{nc} = 3 * h_{ef} * (c_{a1} + 1{,}5 * h_{ef})$ and c_{a1} is the edge distance.

$A_{nco} = 9 * {h_{ef}}^2$

To compute failure in steel, ACI318 [10] and CEB [11] assumed a tensile failure of the shank and recommended the following equation:

$$Q_{sa} = n * A_s * f_u \tag{5}$$

where n is the number of studs.

By contrast, the design shear resistance of an automatically welded headed stud is determined in EC-4 [26] from:

$$Q = \frac{0.8 \cdot f_u \cdot A_s}{\gamma_v} \tag{6}$$

or:

$$Q = \frac{0.29 \cdot \alpha \cdot d^2 \sqrt{f_{ck} E_{cm}}}{\gamma_v} \tag{7}$$

whichever is smaller, with

$$\alpha = 0.2 \cdot \left(\frac{h_{ef}}{d} + 1\right) \text{ for } 3 \le h_{ef} \le 4 \tag{8}$$

$$\alpha = 1 \text{ for } h_{ef} \ge 4 \tag{9}$$

where:

γ_v is the partial factor, which equals 1 in this verification
d is the diameter of the stud shank, 16 mm≤ d ≤ 25 mm
f_u is the specified ultimate tensile strength of the stud's material, but this is no higher than 500N/mm^2.

According to AISC360 [8], steel-headed stud anchors subjected only to shear cannot be less than five stud diameters in length. AISC360 [8] precludes concrete failure thanks to the slenderness restrictions and minimum spacing of $3 \cdot h_{ef}$ between anchors to avoid group effects. When concrete breakout strength is not applicable in practice, the design shear strength is determined as follows:

$$Q = f_u \cdot A_s$$

where:

A_{sa} is the cross-sectional area of the headed stud anchor.

It should be noted that EC-4 [26] and AISC360 [8] were not intended specifically for SRCW with edge conditions or for group effects, but rather for composite actions in components in general.

Furthermore, most of the research focusing on the seismic behaviour of SRCW has been conducted in Japan: e.g. Makino [38]. Experiments were run on a single story and single-bay SRCW on an approximately one third scale. From this experimental program, a stud strength formula was recommended to predict the monotonic strength of headed studs in SRCW as:

$$Q = \phi \cdot (0.5 \cdot A_s \sqrt{f_c \cdot E_{cm}}) \tag{10}$$

where $\phi = 0.6 \cdot \phi_1$ is an edge reduction factor, $\phi_1 = \sqrt{a/15}$ and a is the distance from the centre of the stud to the edge of the panel in cm, A_s is the cross-sectional area of the shear stud in cm^2, f_c is concrete compressive strength in kg/cm^2 and E_{cm} is the modulus of concrete in kg/cm^2. This formula is similar to the AISC360 [8] strength formula for those cases in which concrete failure governs, with an additional term, ϕ_1, which aims to reduce the stud capacity for thin walls.

A summary of the shear strength provisions is presented in *Table 8.*

Table 8. Shear Strength Provisions.

Shear Strength	ACI318	AISC360	EC-4	Makino
Concrete	$k_{cp} \cdot N_{cb}$	$A_s * f_u$	$0.29 \cdot \alpha \cdot d^2 \sqrt{f_{ck} E_{cm}}$	$\phi \cdot (0.5 \cdot A_s \sqrt{f_c \cdot E_{cm}}$
Steel	$A_s * f_u$		$0.8 \cdot f_u \cdot A_{sa}$	

Civjan and Singh [17] proposed a modification to the standard push-out test to study the fully reversed cyclic loading of studs. These authors stated that their tests were not specific for any structural element type. They reported that reversed cyclic loading reduced by almost 40% the shear stud capacity compared to static capacities, but they did not report any expression for load-slip curves. NEHPR [39] proposed a reduction factor of strength similar to AISC341 [40], which states that the shear and tensile strengths of headed stud anchors will drop by 25% for seismic designs.

The experimental strength results are compared to the theoretical load obtained from the provisions of ACI318 [10], EC-4 [26], AISC360 [8], AISC341 [40] and Makino [38]. The ratios according to Equation 11 are provided to assess the experimental results.

$$\zeta = \frac{Q_{test}}{Q_{provision}} \tag{11}$$

where:

Q_{test} is the peak load obtained in the test.
$Q_{provision}$ is the predicted load.

The experimental results for both the monotonic and cyclic loadings of all the tests presented herein are shown in *Table 9*.

Table 9. Summary of the experimental results.

Monotonic

					ACI318 / AISC		EC-4		Makino	ACI318		AISC	EC-4		Makino
	Ø (mm)	fc (MPa)	h_{ef}/Ø	Q_{test} (kN)	Concrete *Strength* Q_{cr} *(kN)*	Steel Strength AISC2010 Q_s (kN)	Concrete *Strength* Q_{cr} *(kN)*	Steel Strength Q_s (kN)	Strength *Q* (kN)	Q_{test}/Q_{cr}	Q_{test}/Q_s	Q_{test}/Q_s	Q_{test}/Q_{cr}	Q_{test}/Q_s	Q_{test}/Q_{cr}
1sM	19	24,5	4,68	97,71	104,75	127,59	72,15	102,07	71,43	0,933	0,766	0,766	1,354	0,957	1,368
2sM	19	41,4	4,66	196.07	264,47	255,18	222,11	204,14	142.86	0,741	0,768	0,768	0,883	0,960	1,372
							Prediction: Avg (Max(Q_{test}/Q_{cr},,Q_{test}/Q_s)),			0,851		0,767	1,157		1,370
							Standard Deviation:			0,116		0,002	0,278		0,003

Cyclic

					ACI318 / AISC		EC-4		Makino	ACI318		AISC	EC-4		Makino
	Ø (mm)	fc (MPa)	h_{ef}/Ø	Q_{test} (kN)	Concrete *Strength* Q_{cr} *(kN)*	Steel Strength AISC2010 Q_s (kN)	Concrete *Strength* Q_{cr} *(kN)*	Steel Strength Q_s (kN)	Strength *Q* (kN)	Q_{test}/Q_{cr}	Q_{test}/Q_s	Q_{test}/Q_s	Q_{test}/Q_{cr}	Q_{test}/Q_s	Q_{test}/Q_{cr}
1sC	19	24,5	4,68	67,34	104,35	127,59	72,15	102,07	71.43	0,645	0,528	0,528	0,933	0,660	0,943
2sC	19	24.5	4,66	140.3	206.95	255.18	144.3	204,14	142.86	0,678	0,550	0,550	0,972	0,687	0,982
							Prediction: Avg (Max(Q_{test}/Q_{cr},,Q_{test}/Q_s)),			0,662		0,539	0,953		0,962
							Standard Deviation:			0,023		0,016	0,028		0,028

In the monotonic tests, and for both the single-stud and two-stud configurations, failures were mixed in steel and concrete. It follows that anchoring studs with slenderness (h_{ef}/d>4.5) is suitable against shear forces to reach failure in steel. Distances longer than $3 \cdot h_{ef}$ are shown to be suitable in order to avoid the interaction between studs in strength terms. No group effects were noted in terms of strength since specimen 2sM (2 studs) reached a peak load of 196.07kN, while specimen 1sM (1 stud) failed at 97.71kN.

When the cyclic and monotonic experimental results are compared (*Table 9*), strength was lower in the cyclic tests than in the monotonic tests. Due to cyclic loading, reduction factors of 0.69 ($= \frac{Q_{test,C16}}{Q_{test,M18}}$) (in the single stud configuration) and 0.71 ($= \frac{Q_{test,C3}}{Q_{test,M6}}$) (for the two-stud configuration) were obtained. As no group effects appeared in the two-stud configuration, an average reduction factor of 0.70 may be proposed to design studs installed in SRCW.

Based on the predictions made in the monotonic tests, the EC-4 [26] prediction provided a better approach with a conservative result. The predictions made for steel strength by ACI318 [10] and AISC360 [8] were unsafe, but the partial safety factor (0.65) provided conservative results. EC-4 [26], together with Makino's expression, presented better approaches with the expression that predicted failure in concrete than in steel. This approach provided suitable results because a mixed failure type was found between steel and concrete while testing.

4. Conclusions

A new test setup for SRCW was designed to examine the real conditions of the studs related force type (shear, tensile, monotonic and cyclic loading), edge conditions and group effects. The following conclusions may be drawn:

1. The experimental load-slip curves obtained by the proposed test are not adjusted for stiffness (half the stiffness was obtained) to the expressions found in the literature. Current expressions available in the literature to predict the stiffness were usually calibrated with standard push-out tests. The test setup showed in this work, allows for the analysis of the stiffness of the connection that studs establish for the edge conditions of a SRCW.

2. The ductility index drops considerably when two studs are installed as compared to the test with a single stud given the heavier load derived in the test and consequent concrete degradation (splitting cracks).

3. Similar to the monotonic tests, the prediction for stiffness in the cyclic tests is much higher (double) than that obtained in the proposed test because the modified push-outs, from which these expressions derive, do not reproduce the typical edge conditions and group effects of the studs installed in SRCW.

4. A reduction factor of 0.70 for the shear strength of studs is needed to accurately predict the peak load of the cyclic tests compared to the monotonic ones for the specimens presented herein.

5. ACI318 [10], AISC360 [8], EC-4 [26] and Makino's formulae [38] were assessed with the experimental test presented herein. AISC360 [8] and ACI318 [10] require a factor between 0.539 and 0.662 to take into account cyclic behaviour if designers use these provisions. EC-4 [26] and (Makino [38]) overestimate by 5% the strength prediction of cyclic loading when monotonic predictions are made.

Having validated the test setup with four specimens, more experimental specimens should be used to check and extend the conclusions drawn regarding the reduction factors for the cyclic design of studs, group effects on stiffness and the slenderness effect of studs (h_{ef}/d).

Acknowledgments

The present study was supported by the Universitat Politècnica de València (UPV) and the Spanish Ministry of Economy and Competitiveness through Project BIA2015-70651-R and Generalitat Valenciana (GVA) by BEST2018. The authors would like to express their gratitude to Debra Westall for revising the manuscript.

References

[1] Dall'Asta, A. Leoni, G. Morelli, F., Salvatore, W. and Zona, W. An innovative seismic-resistant steel frame with reinforced concrete infill walls. Engineering Structures, Volume 141, 15 June 2017. 144-158.

[2] Morelli, F., Caprili, S. and Salvatore, W. Dataset on the cyclic experimental behavior of Steel frames with Reinforced Concrete infill Walls. Data in Brief Open Access Volume 19, August 2018, Pages 2061-2070.

[3] Morelli, F., Mussini, N. and Salvatore, W. Influence of shear stud distribution on the mechanical behavior of dissipative hybrid steel frames with r.c. infill walls. Bulletin of Earthquake Engineering Volume 17, Issue 2, 15 February 2019, Pages 957-983.

[4] Zhuang, B. and Liu, Y. Study on the composite mechanism of large Rubber-Sleeved Stud connector. Construction and Building Materials, Volume 53, 28 February 2014. 533-546.

[5] Yan, J.B., Wang, Z., Wang, T. and Wang, X.T. Shear and tensile behaviors of headed stud connectors in double skin composite shear wall. Steel and Composite, An International Journal. 2018. 26 (6), 759-769. Techno-Press.

[6] Peng, XT and Gu, Q. Seismic behavior analysis for composite structures of steel frame-reinforced concrete infill wall. Structural design of tall and special buildings. 22 (11). 2013. 831-846.

[7] Naseri, N and Behfarnia, K. A numerical study on the seismic behavior of a composite shear wall. Computers and Concrete, An Int'l Journal. 2018. Vol. 22 No. 3..

[8] AISC360. Load and Resistance Factor Design Specification for Structural Steel Buildings, American Institute for Steel Construction. Chicago, Illinois. 2016.

[9] Yan Jia-Bao, Zhong-Xian Li and Wang Tao. Seismic behaviour of double skin composite shear walls with overlapped headed studs". Construction and Building Materials, Volume 191, 10 December 2018. 590-607.

[10] ACI318. Building code requirements for structural concrete (ACI318) and commentary (ACI318R). Farmington Hills, Michigan. 2008.

[11] Comite Euro-International du Beton - CEB. Fastenings to concrete and masonry structures. State of the art report. Bulletin 216, 1994. Telford, London.

[12] Pallarés, L. and Hajjar, J. F. Headed steel stud anchors in composite structures, Part I: Shear. Journal of Constructional Steel Research (Elsevier) 66, no. 2: 198-212. 2010.

[13] Hawkins, N.M. and Mitchell, D. Seismic response of composite shear connections. Journal of Structural Engineering (ASCE*),* 110, 1984. no. 9: 1-10.

[14] Gattesco, N. and Giuriani, E. Experimental study on stud shear connectors subjected to cyclic loading. Journal of Constructional Steel Research*,* 38, 1996. no. 1: 1-21.

[15] Bursi, O S, and Ballerini, M. Behavior of a steel–concrete composite substructure with full and partial. Proceedings of the Eleventh World Congress on Earthquake Engineering. Acapulco: Elsevier. 1996. Paper 771.

[16] Zandonini, R, and Bursi, O.S. Cyclic behavior of headed shear stud connectors. Edited by J F Hajjar, M Hosain, W S Easterling and B M Shahrooz. Composite construction in steel and concrete IV. Reston: ASCE. 470–82. 2002.

[17] Civjan, Scott A. and Prabhjeet Singh. Behavior of shear studs subjected to fully reversed cyclic loading. Edited by ASCE. Journal of Structural Engineering, ASCE. 2003. 1466-1474.

[18] Fa-xing Ding, Guo-an Yin, Hai-bo Wang, Liping Wang and Qiang Guo. Behavior of headed shear stud connectors subjected to cyclic loading. Steel and Composite Structures, An Int'l Journal 2017. **25.** 6.

[19] Viest, I.M. Investigation of stud shear connectors for composite concrete and steel T-beams. Journal of ACI 1956; 27(8);875-91.

[20] Jianan Qi, Jingquan Wang, Ming Li and Leilei Chen. Shear capacity of stud shear connectors with initial damage: Experiment, FEM model and theoretical formulation. Steel and Composite Structures, An Int'l Journal. 2017. Vol. 25 No. 1..

[21] Yu-Liang He, Xu-Dong Wu, Yi-Qiang Xiang, Yu-Hang Wang, Li-Si Liu and Zhi-Hai He. Mechanical behavior of stud shear connectors embedded in HFRC. Steel and Composite Structures, An Int'l Journal. 2017. Vol. 24 No. 2.

[22] Shariati, A., Shariati, M., Sulong, N.H., Suhatril, M. and Mahoutian, M. Experimental assessment of angle shear connectors under monotonic and fully reversed cyclic loading in high strength concrete. Construction and Building Materials, Volume 52, 15 February 2014. 276-283.

[23] Shariati, M, Ramli Sulong, N.H., Suhatril, M., Shariati, A., and Sinaei, H. Comparison of behaviour between channel and angle shear connectors under monotonic and fully reversed cyclic loading. Construction and Building Materials, Volume 38, January 2013, Pages 582-593.

[24] Bezerra, L. M., Barbosa, W. C. S., Bonilla, J. and Cavalcante, O.R.O. Truss-type shear connector for composite steel-concrete beams. Construction and Building Materials, Volume 167, 10 April 2018, Pages 757-767.

[25] Spremic, M., Pavlovic, M., Markovic, Z., Veljkovic, M. and Budjevac, D. FE validation of the equivalent diameter calculation model for grouped headed studs. Steel and Composite, An International Journal. 2018. 26 (3), Techno-Press.

[26] Eurocode 4, UNE - ENV 1994-1.1. Design of composite steel and concrete structures. Part 1-1: General. Common rules and rules for buildings. AENOR. 2004.

[27] Krawinkler, H., Gupta, A., Medina, R., and Luco, N. Development of Loading Histories for Testing of Steel Beam-to-Column Assemblies. Standford University, Standford. 2000.

[28] FEMA-461. Interim Testing Protocols for Determining the Seismic Performance Characteristics of Structural and Nonstructural Components. Redwood City, California. 2007.

[29] Wang, J., Qi, J., Tong, T. Xu, Q and Xiu H. Static behavior of large stud shear connectors in steel-UHPC composite structures. Engineering Structures, 178. 2018. 534-542.

[30] Burnet, O. and Oehlers, D.J. Fracture of mechanical shear connectors in composite beams, Mechanics of Structures and Machines, Vol. 29, No. 1, 2001, 1–41.

[31] Oehlers, D.J. and Coughlan, C.G. The shear stiffness of stud shear connections in composite beams, J. Constr. Steel Res. 6 (4). 1986. 273–284.

[32] Ollgaard J.G., Slutter R.G. and Fisher J.W. Shear strength of stud connectors in light-weight and normal-weight concrete. *AISC Eng J.* 1971; 8(2):55–64.

[33] Ann, L., and Cederwall, K. Push-out tests on studs in high strength and normal strength concrete. Journal of Constructional Steel Research, 1996; 36(1):15–29.

[34] Xue, W.C., Ding, M., Wang, H. and Luo, Z.W. Static behavior and theoretical model of stud shear connectors. J Bridge Eng. 2008;13(6):623–34.

[35] Wang, L., Webster, M.D. and Hajjar, J.F. Pushout tests on deconstructable steel-concrete shear connections in sustainable composite beams. Journal of constructional steel research, 153.Elsevier. 2019. 618-637.

[36] Buttry, K. E. Behaviour of stud connectors in lightweight and normal-weight concrete. M.S. Thesis (unpublished), University of Missouri, USA, August 1965.

[37] Classen, M. and Hegger, J. Shear-slip behaviour and ductility of composite dowel connectors with pry-out failure. Engineering Structures, 150. Elsevier. 2017. 428-437.

[38] Makino, M. Design of framed steel structures with infill reinforced concrete walls. Edited by Roeder CW. ASCE. New York: ASCE. 1985. 279-87.

[39] NEHPR. Recommended Seismic Provisions for New Buildings and Other Structures. 2015 Edition.

[40] AISC341. Seismic Provisions for Structural Steel Buildings. American Institute for Steel Construction. Chicago, Illinois. 2016.